

Deposition and transport of gold by thiosulphates, Veitsch, Austria

H. KUCHA

Institute of Geology and Mineral Deposits, Ave. Mickiewicza 30, 30-059 Kraków, Poland

W. PROHASKA AND E. F. STUMPFEL

Institute of Geological Sciences, Mining University, A-8700 Leoben, Austria

Abstract

Two types of gold can be distinguished in tetrahedrite from the Veitsch magnesite deposit, Austria. Primary gold present in unfractured massive tetrahedrite, has a grain size up to 18 μm and contains, on average, Cu 8.73, Ag 7.01, Au 78.63 and Hg 2.35 (wt.%). Secondary gold is present in fractures and is directly intergrown with digenite, covellite, Cu-thiosulphate, cuprite and chrysocolla but not with malachite or azurite. The secondary gold is up to 200 μm in size with an average composition of Cu 3.06, Ag 6.82, Au 86.41 and Hg 3.51 (wt.%). It is usually closely intergrown with thiosulphates containing up to 0.21 wt.% Au. This, together with the presence of 'dirty' gold with cloudy thiosulphate inclusions, directly indicates the transport and deposition of Au by a thiosulphate ligand. We believe this is the first reported direct evidence of gold transport and deposition by thiosulphate complexes in a natural environment.

KEYWORDS: gold, tetrahedrite, magnesite, thiosulphate, gold transport and deposition, Veitsch deposit, Austria.

Introduction

THE Veitsch magnesite deposit belongs to a group of similar deposits occurring in the Northern Greywacke Zone (NGWZ) of the Eastern Alps. This zone reaches a maximum width of 30 km but extends from the Semmering in the East to the Arlberg area in the West over a distance of almost 400 km (Fig. 1). The NGWZ is strongly mineralized with Fe, Cu, Ag, etc., and was the basis for intensive mining activities in the Middle Ages. Metalliferous mining has been discontinued and only magnesite and talc are mined at present. Magnesite bodies similar to that at Veitsch occur throughout the NGWZ from Semmering in the east to Hochfilzen in the west over a distance of about 250 km.

The Mesozoic rifting and subsequent re-closure due to the collision of the African and European plates since the Middle Cretaceous resulted in appreciable thickening of the continental crust. The Austroalpine nappe system originally formed part of the Adriatic plate overthrust on the Penninic system (European plate). It was divided into three major

nappe systems — the Upper, Middle and Lower Austroalpine (Fig.1). The highest tectonic unit (Upper Austroalpine) originally occupied the southernmost position and was thrust upon the Middle and Lower Austroalpine units. With the exception of the uppermost tectonic units, the Northern Calcareous Alps, these rock series were affected by 'Early Alpine Metamorphism' (cooling ages of about 90 Ma). During a relaxation phase after the peak of Cretaceous metamorphism, mineralization occurred in connection with quartz veining. The NGWZ is the crystalline basement of the Upper Austroalpine Unit underlying the unmetamorphosed series of the Mesozoic Northern Calcareous Alps and comprise mainly Palaeozoic volcano-sedimentary sequences including metavolcanics (greenschists), phyllites and carbonates. The tectonically underlying crystalline units of the Central Alps in the south consist of polymetamorphic series (Variscan amphibolite-facies metamorphics with greenschist facies overprinting during Cretaceous metamorphism).

The magnesite bodies are hosted in Carboniferous strata of the NGWZ metamorphosed in greenschist

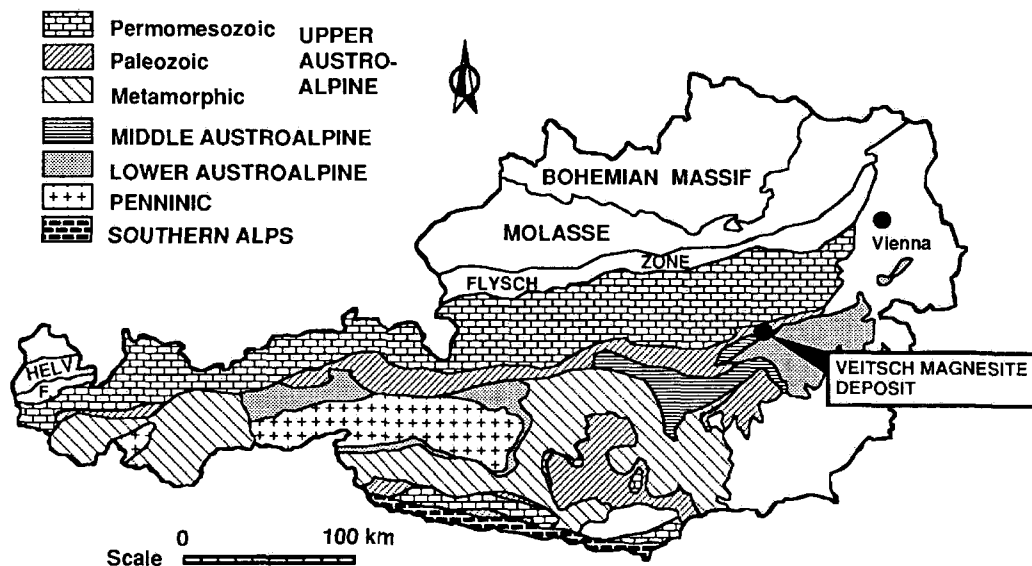


FIG. 1. Simplified, general geological map of Austria showing location of the Veitsch magnesite deposit.

facies during the 'Early Alpine Metamorphism' of Upper Cretaceous age. The magnesite is assumed to have formed syngenetically in a subtidal environment with later modification during diagenesis (Pohl, 1990). An epigenetic origin during late diagenesis or early metamorphism where calcium carbonates would be replaced by hydrothermal Mg-rich solutions derived from ophiolitic complexes, submarine volcanism or connate waters have also been advocated (Holzer, 1986).

In the Veitsch open pit tetrahedrite occurs in close association with quartz–dolomite veinlets cutting the magnesite body. Where it crops out at the surface, tetrahedrite is invariably associated with weathering products, i.e. malachite and azurite. The fact that the veins are unmetamorphosed indicates the formation of these structures after the peak of the Cretaceous metamorphism (approx. 90 Ma).

The S-K α and S-K β emission X-ray lines show systematic shift depending on sulphur valence, and the S-K β line exhibits valence related satellites. The above valence shifts are large enough to be measured by microprobe spectrometers (Kucha *et al.*, 1989). A double S-K β peak related to S²⁻ and S⁶⁺ is resolved in thiosulphates, and the data reported in this note are based on the application of the above method.

Materials and methods

Trace elements were analysed by Atomic Absorption spectrometry (Ag, Pb), Fire Assay (Au) and Mass

Spectroscopy (Pd, Pt). Microprobe analyses were carried out on an ARL SEMQ probe at 25 kV using the following X-ray lines and synthetic standards: S-K α , Fe-K α , Cu-K α and Sb-L α (Cu₁₁FeSb₄S₁₃), (ZnS), As-K α (Cu₁₁FeAs₄S₁₃), Ag-L α , Au-L α , Hg-L α (HgSe) and Bi-L α (Bi₂S₃).

Oxygen was measured using the O-K α line at 10 kV using Fe₂O₃ as a standard. The valence of sulphur was determined with a PET stepped over 20 spectrometer units, dwell time of 10 s/step and cubic FeS₂ as a zero reference point (Kucha *et al.*, 1989). Fine scans of the S-K β peak top were made stepping over two spectrometer units with a dwell time of 4 s.

Mineral separates of quartz were analysed for $\delta^{18}\text{O}$ using the bromine pentafluoride extraction technique described by Clayton and Mayeda (1963). The δD analyses of the fluid inclusions from quartz were done by decrepitation of acid-washed, dried and outgassed quartz at 1100°C. Zinc was used for reduction of the water to H₂ for isotopic analyses. The $\delta^{18}\text{O}$ and δD values are normalized to SMOW.

Geochemistry of tetrahedrite

Tetrahedrite occurs in the Veitsch deposit as minor veinlets and nests up to 20 cm in diameter within the massive magnesite body. Tetrahedrite is often associated with chalcopyrite and minor arsenopyrite. In outcrops of the Veitsch quarry, tetrahedrite is invariably accompanied by its weathering products

TABLE 1. Trace element composition of the Veitsch tetrahedrite (Au, Pd, Pt — ppb; Ag, Pb — ppm)

Sample	Au	Ag	Pd	Pt	Pb
1A	13,500	740	3	4	14
2B	12,500	460	3	3	16
3B-alt	4,000	68	6	7	6
4F	13,000	880	3	3	10
CH	13,000	740	3	3	10
MDL	1	1	1	1	2

MDL — Minimum Detection Limit.

malachite and azurite. The gold content of the massive tetrahedrite determined by fire assay is very uniform and changes from 12.5 to 13.5 g/t, while the Ag concentration varies between 460 and 880 g/t. The lead content is very low and lies between 6 and 16 ppm (Table 1). The Pd and Pt contents are also very low and vary between 3–6 and 3–7 ppb respectively (Table 1). While mining of magnesite was still in progress at Veitsch, tetrahedrite was considered a useless contaminant and dumped.

Primary gold

Tetrahedrite from the Veitsch quarry is Sb-rich and contains, on average, only 3.15 wt.% of As, 3.20 wt.% of Fe and 0.08 wt.% of Ag. Microareas surrounding inclusions of primary gold are slightly enriched in As and Ag — 3.52 and 0.28 wt.% respectively — and slightly depleted in Fe — 2.88 wt.%. The other elements remain essentially unchanged. The primary gold, up to 18 μm in size, occurs in unfractured massive tetrahedrite and contains more silver and less mercury than its secondary counterpart (Fig. 2).

Secondary gold and its thiosulphate connection

Tetrahedrite is often cut by later fractures filled by weathering products. These are arranged symmetrically from the edge towards the centre in sequence, beginning at the edge: rare chalcocite and common digenite, covellite, Cu-thiosulphate, cuprite, chrysocolla and finally malachite and azurite at the centre. The earliest secondary gold appears as minute grains intergrown with digenite, larger grains (up to 60 μm) are intergrown with covellite and cuprite, whilst the largest grains (up to 200 μm) occur intergrown with thiosulphates and/or Fe-chrysocolla. Grains of secondary gold have not been observed in malachite or azurite. They are also absent in weathering products of chalcopyrite. The secondary gold is

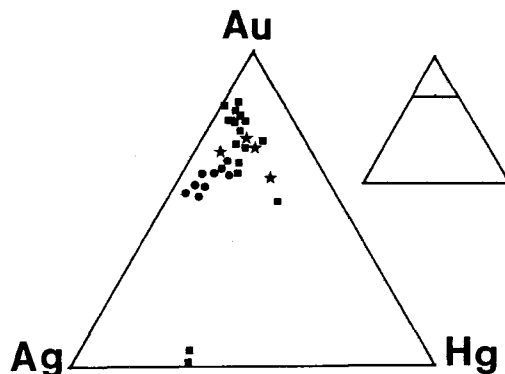


FIG. 2. A triplot of native gold compositions from the Veitsch Quarry. Circles — primary gold; squares — secondary gold; stars — gold with cloudy inclusions.

enriched in Au and Hg compared with the primary gold (Fig. 2). Some secondary gold grains contain dark, cloudy inclusions (Fig. 3) resulting in a 'dirty' appearance under the microscope. This gold contains significant admixtures of S, Cu, As and Sb (Table 2), but it is similar to the secondary gold in its Ag, Au and Hg contents (Fig. 2). Totals of microprobe analyses of 'dirty' gold (Table 2) fall short of 100 % due to the presence of oxygen.

The position of the S-K α peak in 'dirty' gold (Fig. 3) is 0.63 ± 0.07 eV, close to an average valence of S in thiosulphate (Fig. 4). This suggests that dark, cloudy inclusions in gold (Fig. 3) are composed of Cu-thiosulphate (Table 2). The gold grain is rimmed by grey thiosulphate. This compound has a chemical composition close to $\text{Cu}_2\text{S}_2\text{O}_3$ — a copper thiosulphate. The average S valence in this

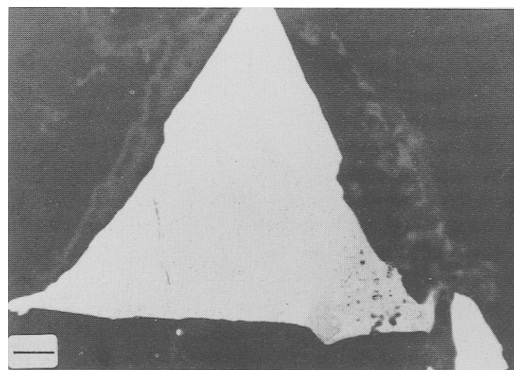


FIG. 3. SEM image of the secondary gold with cloudy thiosulphate inclusions in the right lower corner. Cu-thiosulphate also borders the gold grain to the left and right sides as a wavy grey precipitate. Scale bar: 6 μm .

TABLE 2. Microprobe composition of 'dirty' gold with cloudy inclusions and thiosulphates from the Veitsch deposit (wt.% atomic proportion)

SAMPLE	Si	S	Fe	Cu	Zn	As	Ag	Sb	Au	Hg	O
D1/E1	≤0.05	4.61	1.61	5.11	0.34	2.21	3.99	3.83	71.66	2.15	5.00
D1/E2	2.03	5.82	1.01	8.21	0.82	3.18	2.71	6.12	53.18	4.01	13.50
D1/E3	≤0.05	2.11	0.31	4.08	0.33	1.22	4.37	4.83	73.22	2.78	7.00
D1/F2	0.51	5.17	0.52	7.33	0.41	1.63	6.13	0.64	69.35	2.01	6.50
H218/16A*	0.81 0.0859	21.54 2.0000	9.31 0.4963	40.21 1.8841	2.96 0.1348	2.18 0.0866	0.41 0.0113	3.11 0.0760	0.21 0.0032	0.35 0.0053	19.50 3.6286
H218/A16B*	0.53 0.0502	24.11 2.0000	10.81 0.5148	38.11 1.5954	2.88 0.1172	2.34 0.0831	0.22 0.0054	4.01 0.0876	0.12 0.0016	0.26 0.0034	17.10 2.8428
H218/A16*	2.11 0.3969	12.14 2.0000	14.23 1.3460	41.96 3.4885	3.22 0.2601	2.18 0.1537	0.30 0.0147	7.79 0.3467	0.16 0.0043	0.30 0.0079	16.40 5.4147
H218/A18	1.73 0.3974	9.94 2.0000	14.17 1.6369	33.66 3.4179	3.20 0.3158	1.86 0.1602	0.23 0.0137	10.24 0.5566	≤0.06	≤0.06	25.00 10.0811

* grains analysed by soft X-ray spectroscopy

compound calculated from the sulphur peak shift is 0.69 ± 0.07 eV close to thiosulphate valence 2^+ (Fig. 4). It shows S^{6+} satellite (Fig. 5), a double $S-K\beta$ peak with resolved S^{2-} and S^{6+} components characteristic of thiosulphate (Fig. 6), and it contains from 0.16 to 0.21 wt.% of Au (Table 2).

Stable isotope analyses

In order to identify the type and a nature of the mineralizing hydrothermal fluid the isotopic ratios of oxygen and hydrogen were analysed. The isotopic composition of meteoric water varies with latitude. Low δD and $\delta^{18}O$ values are indicative of higher latitudes or continental environment. Generally the Cretaceous quartz veins in the Eastern Alps seem to be dominated by a lighter δD composition indicating the influence of meteoric water during the formation of these structures (Prochaska, 1993). $\delta^{18}O$ values of hydrothermal fluids equilibrate very quickly with the host rocks and only epithermal fluids in shallow crustal levels may still exhibit their original light oxygen isotope composition. Because of the low hydrogen content in most of the rocks, the original δD values of the migrating fluids are usually well preserved.

The investigated quartz samples yielded consistent $\delta^{18}O$ values of 15 ‰, which is typical for quartz-carbonate veins in greenschist terrains worldwide. Considering the temperature dependence of the oxygen isotope fractionation, this corresponds to a calculated original fluid composition of 7–9 ‰, the

$\delta^{18}O$ assuming a temperature of formation of 300–350°C. The δD composition of the fluid from the inclusions in quartz spans a range from –80 to –90‰.

Discussion

A wide range of anions such as HS^- , Cl^- , Br^- , I^- , $S_2O_3^{2-}$, SCN^- , CN^- and organic complexes can dissolve gold under laboratory conditions (Lakin *et al.*, 1974; Seward, 1993). Under natural regimes chloride and sulphide ligands are abundant and sufficiently stable to account for gold transport and deposition over the temperature range 150–350°C (Seward, 1973; Schenberger and Barnes, 1989). In general, transport in chloride complexes is favoured at low pH, high Cl concentrations and elevated temperatures. At higher pH (but also at low pH when Cl content is low), lower oxygen fugacities, lower Cl concentration, and at lower temperatures, even as low as 25°C (Renders and Seward, 1989) gold can be transported as sulphide complexes. Precipitation of gold from sulphide ligands may be induced by oxidation or reduction of the fluid, i.e. departure from the sulphide-sulphate fence, where the solubility of Au-sulphide complexes is highest, by precipitation of metal sulphides (pyrite, covellite, etc.) and decrease in temperature. All these reactions are sensitive to mineral buffers residing in the country rocks (Schenberger and Barnes, 1989). Experiments show that at low temperatures and low pH, a good solvent for Au and Ag is ferric chloride (Mann, 1984).

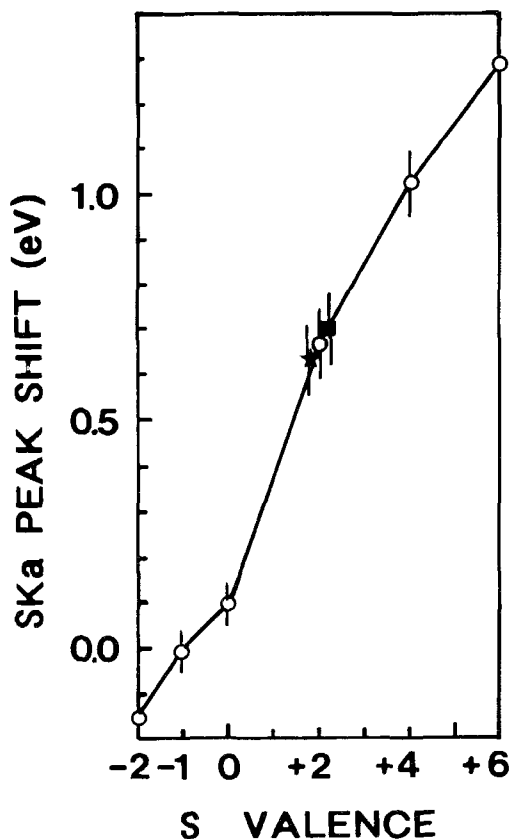


FIG. 4. The relationship between sulphur valence and shift of the S-K α emission line, ARL SEMQ microprobe. PET spectrometer, accelerating potential 20 kV. Open circles — standard specimens of varying sulphur valency: FeS, FeS₂, S, Na₂S₂O₃, CaS₂O₃ and CaSO₄. Star — sample: D1/F2 — gold with cloudy inclusions (Fig. 2, Table 2), square — sample H218/A16A — copper thiosulphate Table 2.

Thiosulphate is a good solvent for Au and Ag at neutral and alkaline pH range. Under similar conditions bicarbonate-sulphide complexes dissolve Au efficiently but only minor quantities of Ag enter the fluid (Mann, 1984).

In the case of the Veitsch deposit, the secondary weathering gold has been derived from the primary Au residing in the tetrahedrite. There are three possible transporting ligands to consider during remobilization: sulphide, bicarbonate-sulphide and thiosulphate. Thiosulphate at the Veitsch deposit seems to be the best choice given the observed paragenesis and geochemistry of the secondary minerals where chlorine is absent. There are two

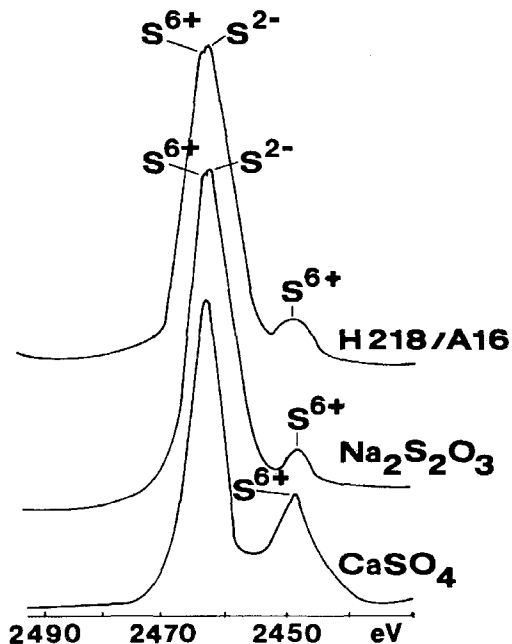


FIG. 5. Scan of the S-K β line in the CaSO₄ and Na₂S₂O₃ standards and in copper thiosulphate showing the valency-related S⁶⁺ satellite.

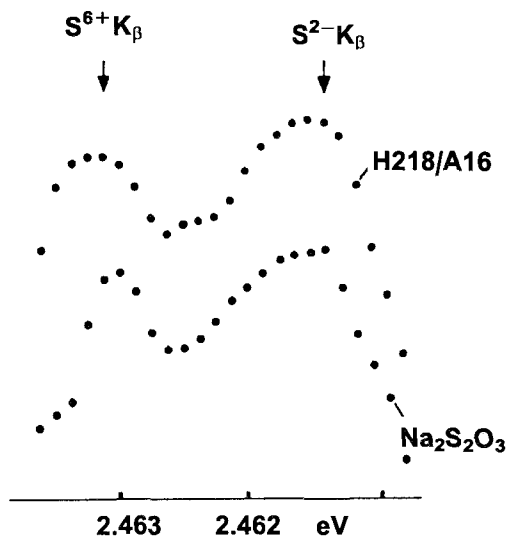


FIG. 6. Fine scan of the S-K β peak top in thiosulphate standard and in the studied copper thiosulphate showing resolved S⁶⁺ and S²⁻ components. ARL SEMQ microprobe, PET spectrometer, 20 kV.

reasons for this view: (1) thiosulphates are closely associated with gold and contain 0.16–0.21 wt.% of refractory gold (Table 2), and (2) thiosulphates form cloudy inclusions in grains of secondary gold (Fig. 3). There are two possible mechanisms of precipitation of Au from thiosulphatic solutions (complexes). (1) Disproportionation of $S_2O_3^{2-}$ into sulphide and sulphate. This could explain a precipitation of Au in a close association with digenite, gold and covellite. Sulphate remaining in the solution is a poor solvent of gold (Mann, 1984). (2) Oxidation of $S_2O_3^{2-}$ to $2SO_4^{2-}$ with a subsequent drop in pH. The former mechanism could cause a precipitation of gold, the later precipitation of silica, thus explaining the observed close association of gold with chrysocolla.

Thiosulphates are stable close to the sulphide–sulphate fence at neutral and elevated pH (Valensi *et al.*, 1963). This is exactly the regime where gold sulphide complexes attain the highest solubility (Seward, 1973; Schenberger and Barnes, 1989). Thiosulphates are stable up to about 250°C (Kucha and Viaene, 1993) and, therefore, they could also compete with chloride and sulphide ligands to carry gold at elevated temperatures. More sulphur is dissolved as thiosulphate than as sulphide or as sulphate in the hot springs in New Zealand, and this may be considered evidence in support of the above considerations (Webster, 1987).

From the geological point of view, magmatic and epithermal fluids can be ruled out as a source for the Veitsch quartz–fahlore veins. The observed isotope numbers can be accounted for by meteoric fluid modified by interaction with the host rock, especially as regards the oxygen isotope composition. The possibility of an admixture of small amounts of deep fluids (metamorphic devolatilization fluids or formation water from tectonically deeper sedimentary units) cannot be excluded. Such fluids are likely to have been mobilized during a relaxation phase following the peak of the Early Alpine Metamorphism, resulting in vein type mineralizations in shallow crustal levels where the hydraulic regime is dominated by meteoric water. This is also an environment with conditions favourable for thiosulphate stability; isotopic evidence can thus be considered as supporting the concept of thiosulphates as significant agents in low-temperature gold mineralization.

Acknowledgements

We are indebted to H. Mühlhans, Institute of Geological Sciences, Leoben, for help during microprobe work. We are grateful to The Austrian Academy of Sciences, Commission for Basic Research on Mineral Raw Materials for generous support of this project.

References

- Clayton, R. N. and Mayeda, T. K. (1963) *Geochim. Cosmochim. Acta*, **27**, 43–52.
- Holzer, H. F. (1986) Austria. 15–40. In *Mineral Deposits of Europe*, vol. 3, Central Europe (Dunning, F.W. and Evans, A.M., eds.) 355 pp. Inst. Min. Metall. and Mineral. Soc. London.
- Kucha, H., Wouters, R. and Arkens, O. (1989) *Scanning Microscopy Int.*, **3**, 89–97.
- Kucha, H. and Viaene, W. (1993) *Min. Deposita*, **28**, 13–21.
- Lakin, H.W., Curtin, G. C., Hubert, A. E., Shackette, H.T. and Dostader, G. (1974) *US Geol. Surv. Bull.* **1330**, 80 pp.
- Mann, A. W. (1984) *Econ. Geol.*, **79**, 38–49.
- Pohl, W. (1990) *Geologische Rundschau*, **79**, 291–9.
- Prochaska, W. (1993) *Berg. Hütten. Monatsch.*, **4**, 138–44.
- Renders, P. J. and Seward, T. M. (1989) *Geochim. Cosmochim. Acta*, **53**, 245–53.
- Seward, T. M. (1973) *Geochim. Cosmochim. Acta*, **37**, 379–99.
- Seward, T. M. (1993) The hydrothermal geochemistry of gold. 37–62. In *Gold Metallogeny and Exploration* (Foster, R.P., ed.) Chapman & Hall. 432 pp.
- Schenberger, D. M. and Barnes, H. L. (1989) *Geochim. Cosmochim. Acta*, **53**, 269–78.
- Valensi, G., Muylder Van, J. and Pourbaix, M. (1963) Soufre. In *Atlas d'Equilibres Electrochimiques, 25°C* (Pourbaix, M., Zubov de, N. and Muylder Van, J., eds.) Gauthier-Villars, Paris, 545–53.
- Webster, J. G. (1987) *Appl. Geochem.*, **2**, 579–84.

[Manuscript received 10 January 1994;
revised 17 August 1994]